NASA TECHNICAL MEMORANDUM

NASA TM X-3395

NASA TM X-3395

EFFECT OF COOLANT FLOW EJECTION ON AERODYNAMIC PERFORMANCE OF LOW-ASPECT-RATIO VANES

I - Performance With Coolant Ejection Holes Plugged

Jeffrey E. Haas and Milton G. Kofskey

Lewis Research Center
and U.S. Army Air Mobility R&D Laboratory
Cleveland, Ohio 44135

NATIONAL AERONAUTICS AND SPACE ADMINISTRATION • WASHINGTON, D. C. • APRIL 1976

1. Report No.	2. Government Accession No.	3. Recipient's Catalog No.
TM X-3395		

4. Title and Subtitle	5. Report Date
EFFECT OF COOLANT FLOW EJECTION ON AERODYNAMIC PERFORMANCE OF LOW-ASPECT-RATIO VANES I - PERFORMANCE WITH COOLANT EJECTION HOLES PLUGGED	April 1976
	6. Performing Organization Code

7. Author(s)	8. Performing Organization Report No.
Jeffrey E. Haas and Milton G. Kofskey	E-8611
	10. Work Unit No. 505-04

9. Performing Organization Name and Address	11. Contract or Grant No.
NASA Lewis Research Center and U.S. Army Air Mobility R&D Laboratory Cleveland, Ohio 44135	
	13. Type of Report and Period Covered
12. Sponsoring Agency Name and Address	Technical Memorandum
National Aeronautics and Space Administration Washington, D.C. 20546	14. Sponsoring Agency Code

15. Supplementary Notes

16. Abstract

The aerodynamic performance of a low aspect ratio turbine vane designed with coolant flow ejection holes on the vane surfaces was experimentally determined in a full-annular cascade with the coolant ejection holes plugged. The purpose was to establish a baseline for comparison with tests where flow is ejected from the vane surfaces. The vanes were tested over a mean-section ideal critical velocity ratio range of 0.64 to 0.98. This ideal critical velocity ratio corresponds to the vane inlet total to vane aftermixed static pressure ratio at the mean section. The variations in vane efficiency and aftermixed flow conditions with circumferential and radial position were obtained.

17. Key Words (Suggested by Author(s))	18. Distribution Statement
Aerodynamic performance Annular cascade Secondary flow Cooled vanes	Unclassified - unlimited STAR Category 02

19. Security Classif. (of this report)	20. Security Classif. (of this page)	21. No. of Pages	22. Price*
Unclassified	Unclassified	17	$3.25

* For sale by the National Technical Information Service, Springfield, Virginia 22161

EFFECT OF COOLANT FLOW EJECTION ON AERODYNAMIC PERFORMANCE OF LOW-ASPECT-RATIO VANES

I - PERFORMANCE WITH COOLANT EJECTION HOLES PLUGGED

by Jeffrey E. Haas and Milton G. Kofskey

Lewis Research Center and
U.S. Army Air Mobility R&D Laboratory

SUMMARY

The aerodynamic performance of a low aspect ratio turbine vane designed with coolant flow ejection holes on the vane surfaces was experimentally determined in a full-annular cascade with the coolant ejection holes plugged. The purpose of this test was to establish a baseline for comparison with tests where flow is ejected from the vane surfaces. The first-stage gas generator turbine vanes from the GE-12 demonstrator engine were used as test vanes. The vanes were tested over a mean-section ideal critical velocity ratio range of 0.64 to 0.98. This ideal critical velocity ratio corresponds to the vane inlet total to vane aftermixed static pressure ratio at the mean section. The design value of the mean-section ideal critical velocity ratio for the vane is 0.894. Annular surveys were made downstream of the vane trailing edge for this range of mean-section ideal critical velocity ratio. The variations in vane efficiency and aftermixed flow conditions with circumferential and radial position were obtained.

A total pressure ratio contour plot at the vane exit survey plane indicated the presence of thick, deep wakes extending well away from both sides of the trailing edge. The thick wakes are believed to be caused by secondary flow which moves low momentum fluid cross channel on the outer wall from the pressure to the suction surface and radially in the vane wakes.

The loss due to secondary flow was isolated from the total vane loss. Calculations indicated that the secondary flow accounted for approximately 32 percent of the total vane loss.

INTRODUCTION

Advanced small turboshaft engines in the 1.00 to 4.50 kilogram per second, 250 to 1100 kilowatt class are being designed to operate at cycle pressure ratios of 10 to 1 or higher, with turbine inlet temperatures as high as 1550 K. The high compressor pressure ratio, together with the small mass flow, results in a turbine design with a small annulus area and, therefore, a small blade height. A high turbine inlet temperature requires the use of blade cooling air, and, therefore, the stator and rotor blade profiles must be fabricated longer and thicker than desired from an aerodynamic standpoint to provide adequate space for cooling passages. Long chord lengths and small blade heights result in a low aspect ratio design.

Reference 1 indicates that low aspect ratio designs have significantly greater secondary flow losses than high aspect ratio designs because the secondary flow fields encompass a significantly greater proportion of the airflow channel. Reference 2 showed experimentally that low momentum fluids on the blade surfaces and endwalls and in the blade wakes are transported radially and circumferentially to form cores of high losses. Blade cooling can compound this problem because low momentum coolant flow being ejected from holes and slots can significantly increase boundary layer and blade wake thickness. This increased boundary layer and blade wake thickness can also be transported into secondary loss cores to further increase the total vane loss.

To study the effect on performance of coolant flow ejection from the surfaces of a small turbine vane, an experimental investigation consisting of radial and circumferential surveys of flow angle and total pressure was conducted on the first-stage gas generator turbine vanes from the GE-12 demonstrator engine in a full-annular cascade. In order to establish a basis for evaluating the effect on performance of coolant flow ejection, a baseline performance with the coolant holes plugged flush with the vane surfaces to prevent internal flow circulation and surface flow disturbances was first determined. The second phase will be to determine the performance of the vane cascade with coolant flow ejection with a primary to coolant temperature ratio of 2. The vane had a blade height of 1.75 centimeters and an aspect ratio of about 0.5.

This report describes the baseline performance tests and results. The baseline tests were conducted over a mean-section ideal critical velocity ratio range of 0.64 to 0.98. This ideal critical velocity ratio corresponds to the vane inlet total to vane exit aftermixed static pressure ratio at the mean section. The design value of the ideal critical velocity ratio at the mean section is 0.894. Annular surveys were made downstream of the vane trailing edge for this range of mean-section critical velocity ratios.

SYMBOLS

p	pressure, N/cm^2
R	gas constant, J/(kg)(K)
r	radial direction, m
T	temperature, K
V	velocity, m/sec
α	flow angle measured from axial direction, deg
γ	ratio of specific heats
$\bar{\eta}$	efficiency at radius r based on kinetic energy
$\bar{\bar{\eta}}$	overall efficiency based on kinetic energy
θ	circumferential direction, deg
ρ	density, kg/m^3
ω	total-pressure-loss coefficient at radius r

Subscripts:

cr	flow conditions at Mach 1
i	survey position closest to inner (hub) wall
id	ideal or isentropic
mean	mean radius
o	survey position closest to outer (tip) wall
u	tangential direction
z	axial direction
1	station at vane inlet (fig. 5)
2	station downstream of vane trailing edge where total pressure measurements were taken (fig. 5)
2a	station downstream of vane trailing edge where angle measurements were made (fig. 5)
3	station downstream of vane trailing edge where static pressures were measured (fig. 5)
3M	station downstream of vane trailing edge where flow is assumed to be circumferentially mixed (uniform) (fig. 5)

Superscript:

' total-state condition

APPARATUS

The test apparatus consists of the cascade, the inlet and exhaust piping, and the control valves. A photograph and the cross-sectional view of the facility are shown in figures 1 and 2, respectively. Dry pressurized air from a central supply system flows first through the inlet section, test blading, and then exhausts into a central exhaust system. Control valves at the inlet and exit are used to control the flow conditions upstream and downstream of the test section.

The inlet, consisting of a bellmouth and a short inlet section, provided uniform inlet conditions with small boundary layer growth at the vane inlet.

The test section consists of a full-annular ring of 24 vanes. As shown in figure 2, cooling air can be independently supplied to the vanes through plenums in both endwalls. For the baseline performance investigation reported herein, no blade cooling was employed. Therefore, all the cooling holes and slots in the vane surfaces were plugged flush with the vane surfaces to prevent internal flow circulation and surface flow disturbances. A photograph of 2 two-vane segments is shown in figure 3 before the coolant ejection holes were plugged. There were 12 of these segments in a full-annular ring. These test vanes were the first-stage gas generator turbine vanes from the GE-12 demonstrator engine. The vanes were slightly twisted and have a height of 1.75 centimeters and an axial chord of 2.12 centimeters. The vane aspect ratio and solidity (both based on actual chord length) are about 0.5 and 1.48, respectively. The stator hub to tip radius ratio is 0.82, and the mean radius is 8.67 centimeters. For completeness, the vane velocity diagrams are shown in figure 4.

INSTRUMENTATION

Figure 5 shows station nomenclature and the instrumentation used to measure wall static pressure, total temperature, total pressure, and flow angle. Instrumentation at the vane inlet (station 1) measured static pressure and total temperature. Static pressures were obtained from eight taps with four on the inner wall and four on the outer wall of the annulus. The inner and outer taps were located opposite each other at 90° intervals around the circumference at a distance approximately 1.60 centimeters upstream of the vanes. The temperature was measured with three thermocouple rakes,

each containing three thermocouples at the area center radii of three equal annular areas.

Vane performance was based on measurements obtained from two survey probes located downstream of the vane trailing edge. An angle probe (fig. 6) located at station 2a (fig. 5) was used to determine the variation in flow angle both radially and circumferentially. The angle probe consisted of two parallel tubes with the sending end cut off to form a 90° wedge. Stainless steel tubing with an outside diameter of 0.034 centimeter was used. Station 2a was located approximately 0.63 centimeter downstream of the vane trailing edge. Calibration of this probe showed no sensitivity to Mach number effects up to 0.9.

At station 2, located approximately 0.15 centimeter downstream of the vane trailing edge, a total pressure probe (fig. 7) was installed and positioned at a fixed angle of 73° from the axial direction. This angle is an arithmetical mean of that measured by the angle probe. This angle was subsequently verified to be within 0.5° of the mass-averaged value. The variation in total pressure loss was measured using a differential pressure transducer referenced to the vane inlet static pressure. The total pressure sensing tube was stainless-steel tubing with an outside diameter of 0.034 centimeter. The sensing end of the tube had an inside bevel of 30° to reduce the sensitivity to deviations in ideal flow angle from the average setting. Calibration of this probe showed total pressure measurements were insensitive to deviations in flow angle of $\pm 10^{\circ}$ and Mach number effects up to 0.9. Subsequent angle surveys showed that the maximum angle deviation was only $\pm 5^{\circ}$. The probe element was inclined approximately 25° from the axial direction to obtain measurements near the hub wall. Measurements near the outer wall could also be obtained with this probe because the combined effects of slot width and probe setting angle of 73° allowed the probe tip to be withdrawn all the way to this location.

Circumferentially, the surveys were arbitrarily limited to one blade spacing (15°) as shown in figure 5. The survey area at station 2 (fig. 5) is distorted even though the probe stem covers a true segment of the annulus.

At station 3, located approximately 0.89 centimeter downstream of the vane trailing edge, eight static taps (four each on the inner and outer walls) were spaced at 90° intervals around the circumference. In addition, there were 16 static taps (eight each on the inner and outer walls) located in the same plane. These static taps were spaced at various circumferential positions in order to determine the static pressure variation across the passage. These static taps were installed in several passages because the physical size of the tubing prohibited installation in only one passage. In figure 5 they are rotated into the test channel to illustrate their relative position.

PROCEDURE

Dry pressurized air controlled to a pressure of about 10.34 newtons per square centimeter and 300 K was supplied through control valves. From the cascade the flow was piped into the exhaust system. The exit test conditions were set by controlling the pressure at the vane exit with a throttle valve located in the exhaust system. A tip static tap located downstream of the test section was used to set the pressure ratio.

The baseline tests were conducted over a mean-section ideal critical velocity ratio range of 0.64 to 0.98. This ideal critical velocity ratio corresponds to the vane inlet total to vane exit aftermixed static pressure ratio at the mean section. The design value of the ideal critical velocity ratio at the mean section is 0.894. At a given pressure ratio, data were obtained at 11 different radii over the vane height. At each fixed radius, the probe was moved circumferentially to cover approximately the vane spacing (15°) with data being obtained at discrete points approximately every 1°.

At each discrete point the probe movement was stopped and the probe pressure was allowed to reach equilibrium before taking the data point. The probe pressure was read with a calibrated transducer. All of the transducer signals were digitized and recorded on magnetic tape.

DATA REDUCTION

The baseline performance was calculated from the measurements of total pressure, static pressure, and flow angle. The static pressure was assumed to vary linearly between the hub and tip wall values. The probe angle was maintained at a constant 73°.

The calculation of the vane efficiency is based on the determination of a hypothetical state where it is assumed that the flow has mixed to a circumferentially uniform condition (station 3M). At each radius, the conservation of mass, momentum, and energy is used to obtain this aftermixed state (i.e., $V_{3M,z}(r)$, $V_{3M}(r)$, $T_{3M}(r)$, $\alpha_{3M}(r)$, etc.) from the survey measurements. The calculation procedure is described more fully in reference 3. The aftermixed vane efficiency is used herein because it is theoretically independent of the axial location of the survey measurement plane. It should be noted that the aftermixed efficiency contains not only the vane profile loss but also the mixing loss.

For uncooled vanes, the vane aftermixed efficiency based on kinetic energy can be defined as a function of radius $\overline{\eta}_{3M}(r)$, or as an overall quantity $\overline{\overline{\eta}}_{3M}$, as given by the following equations from reference 3:

$$\overline{\eta}_{3M}(r) = \frac{V_{3M}^2(r)}{V_{3M,id}^2(r)} \tag{1}$$

$$\overline{\overline{\eta}}_{3M} = \frac{\int_{r_i}^{r_o} \rho_{3M}(r) V_{3M,z}(r) V_{3M}^2(r) r \, dr}{\int_{r_i}^{r_o} \rho_{3M}(r) V_{3M,z}(r) V_{3M,id}^2(r) r \, dr} \tag{2}$$

where

$$V_{3M,id}(r) = \sqrt{\left(\frac{2\gamma}{\gamma - 1}\right) RT' \left\{1 - \left[\frac{P_{3M}(r)}{p'}\right]^{(\gamma-1)/\gamma}\right\}} \tag{3}$$

The total pressure-loss coefficient as a function of radius is

$$\overline{\omega}_{3M}(r) = \frac{p_1' - p_{3M}'(r)}{p_1' - p_{3M}(r)} \tag{4}$$

RESULTS AND DISCUSSION

Survey Plane Flow Conditions and Vane Performance

Figure 8 shows the radial variation in the flow discharge angle at a mean-section ideal critical velocity ratio near the design value. The ideal critical velocity ratio corresponds to the ratio of the calculated total pressure at the vane inlet to the vane exit aftermixed static pressure ratio at the mean section. Except for a region near the endwalls, there was underturning in the flow from 0.5° to 2.5°. The maximum deviation from design occurred in regions which were about 20 percent of the vane height from both endwalls. Overturning, which occurred in the flow near the hub wall, was probably caused by endwall cross-channel flow from the pressure to the suction surface. Based on these data, a mass-averaged flow angle of about 73° was determined.

A plot of total pressure ratio contours is shown in figure 9 for a single vane passage at a mean-section ideal critical velocity ratio of 0.895. The projection of the trailing edge to the survey plane, using the experimental flow angles, is also shown in the figure. The lack of repeatability of the pressure contours at the ends of the vane spacing was primarily due to the inability to alining the vane segments together to form circular inner and outer walls without radial steps from one vane segment to another. The dominant feature of figure 9 is the presence of thick, deep wakes extending well away from the trailing edge projection. The lack of a passage vortex or core along the vane suction surface and outer wall suggests that low momentum fluid along the outer wall flows cross-channel from pressure to suction surface and then flows radially inward in the vane wake and contributes to the loss in the vane wake. The region of the low momentum fluid in the corner formed by the vane suction surface and the hub is the result of cross-channel hub boundary layer flow. Low momentum fluid, which flowed radially inward in the blade wake, may have also contributed to this loss region. This type of secondary flow loss pattern was also observed by smoke flow traces as reported in reference 2.

Calculated Aftermixed Flow Conditions and Vane Performance

As discussed in the DATA REDUCTION section, the aftermixed conditions, at each radius, are obtained from the survey measurements by applying the conservation of mass, momentum, and energy to an annulus sector of controlled volume. The variation of aftermixed efficiency $\overline{\eta}_{3M}(r)$ with radial position of a mean-section ideal critical velocity ratio of 0.895 is shown in figure 10(a). A vane efficiency of about 96.5 percent was obtained from about 30 to 70 percent of the vane height. Beyond this range to both endwalls the efficiency dropped off rapidly. This efficiency decrease was due to the large losses associated with the endwall boundary layers. These large losses near the walls are reflected in increased total-pressure-loss coefficients as shown in figure 10(b).

Figure 11 shows the variation in overall efficiency with mean-section ideal critical velocity ratio. The overall efficiency increased from 0.923 at a velocity ratio of 0.634 to 0.933 at a velocity ratio of 0.975. The efficiency at the design mean-section ideal velocity ratio of 0.894 was 0.929.

Secondary Flow Losses

Of particular interest in the study of low aspect ratio turbine vanes is an evaluation of the loss contributed by the secondary flows. One method for isolating this loss

from the total vane loss is as follows. The suction and pressure surface boundary layer parameters can be calculated at the mean radius by using the computer program described in reference 4. The kinetic energy loss coefficient at the mean radius can then be calculated using Stewart's method (ref. 5). The kinetic energy loss coefficient is defined as one minus the efficiency. This solution can be assumed to represent the profile loss over the entire vane height.

Next, the boundary layer on the end walls can be calculated using the inviscid velocity distribution along the mean blade to blade streamlines near the hub and tip walls. The inviscid blade to blade streamline velocity distribution through the vane passage is obtained from the TSONIC computer program (ref. 6). Calculating the end wall boundary growth using reference 4 near the hub and tip walls would be representative of the end wall loss had no secondary flow occurred. The end wall kinetic energy loss coefficient can then be calculated, again using reference 5.

Finally, if the mean-radius and endwall kinetic energy loss coefficients are subtracted from the overall kinetic energy loss coefficient (as calculated from the survey results at the design mean-section ideal velocity ratio of 0.894), the remainder would be the kinetic energy loss coefficient due to secondary flow. Calculations indicated that this kinetic energy loss coefficient due to secondary flow was 0.0227 and represented approximately 32 percent of the total vane loss.

SUMMARY OF RESULTS

The baseline aerodynamic performance of a low aspect ratio vane was experimentally determined in a full-annular cascade. The first-stage gas generator turbine vanes from the GE-12 demonstrator engine were used as test vanes. The vanes were tested over a mean-section ideal critical velocity ratio range of 0.64 to 0.98. This ideal critical velocity ratio corresponds to the vane inlet total to vane exit aftermixed static pressure ratio at the mean section. The design value of the ideal critical velocity at the mean section is 0.894. Annular surveys were made downstream of the vane trailing edge for this range of mean-section ideal critical velocity ratios. The variation in vane efficiency and aftermixed flow conditions with circumferential and radial position were obtained. The results of this investigation are summarized as follows:

1. A total pressure ratio contour plot at the vane exit survey plane indicated the presence of thick, deep wakes extending well away from the trailing edge. These thick wakes were believed to be caused by low momentum fluid along the outer wall being transported cross-channel from the pressure to the suction surface and then radially inward in the vane wakes.

2. The overall aftermixed efficiency at the mean-section ideal critical velocity ratio at 0.894 was 0.929.

3. An analytical method was used to determine the loss due to secondary flow. Calculations indicated that the secondary flow accounted for approximately 32 percent of the total vane loss.

Lewis Research Center,
National Aeronautics and Space Administration,
and
U.S. Army Air Mobility R&D Laboratory,
Cleveland, Ohio, February 2, 1976,
505-04.

REFERENCES

1. Ewen, J. S.; Huber, F. W.; and Mitchell, J. P.: Investigation of the Aerodynamic Performance of Small Axial Turbines. ASME Paper 73-GT-3, Apr, 1973.

2. Rohlik, Harold E.; et al.: Secondary Flows and Boundary-Layer Accumulations in Turbine Nozzles. NACA Rept. 1168, 1954.

3. Goldman, Louis J.; and McLallin, Kerry L.: Cold-Air Annular-Cascade Investigation of Aerodynamic Performance of Cooled Turbine Vanes. I - Facility Description and Base (Solid) Vane Performance. NASA TM X-3006, 1974.

4. McNally, William D.: Fortran Program for Calculating Compressible Laminar and Turbulent Boundary Layers in Arbitrary Pressure Gradients. NASA TN D-5681, 1970.

5. Stewart, Warner L.: Analysis of Two-Dimensional Compressible-Flow Loss Characteristics Downstream of Turbomachine Blade Rows in Terms of Basic Boundary-Layer Characteristics. NACA TN-3515, 1955.

6. Katsanis, Theodore: Fortran Program for Calculating Transonic Velocities on a Blade-to-Blade Stream Surface of a Turbomachine. NASA TN D-5427, 1969.

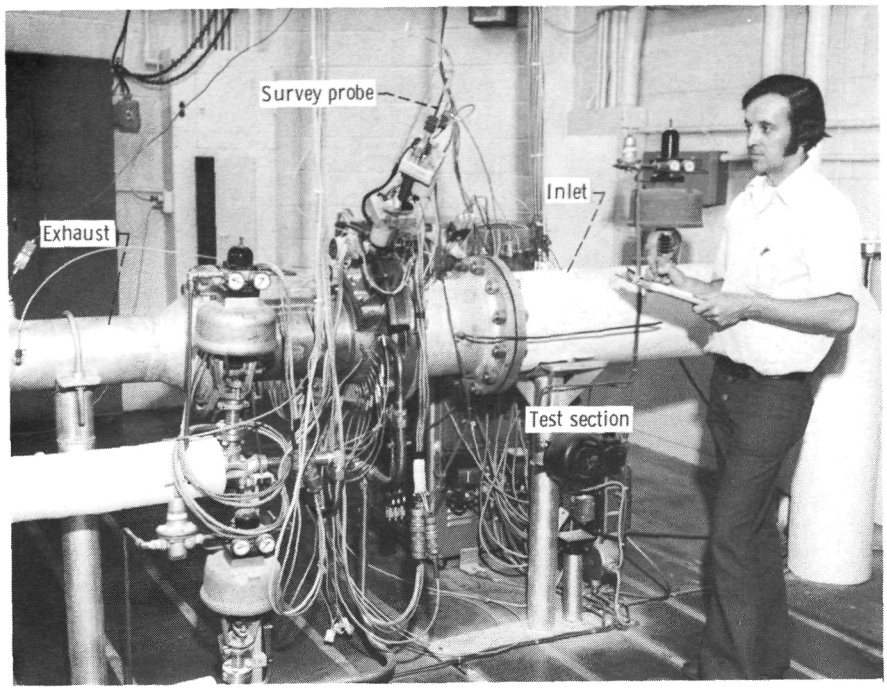

Figure 1. - Test facility.

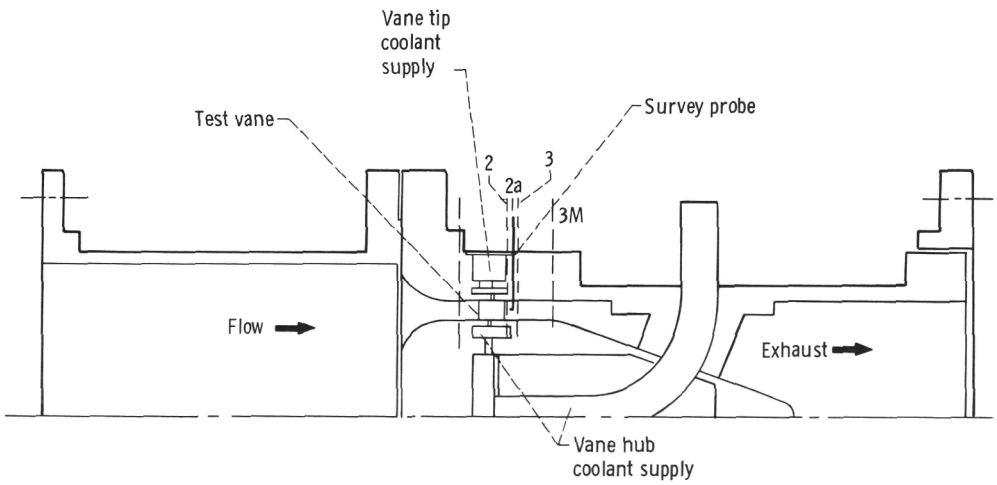

Figure 2. - Schematic cross-sectional view of stator vane cascade.

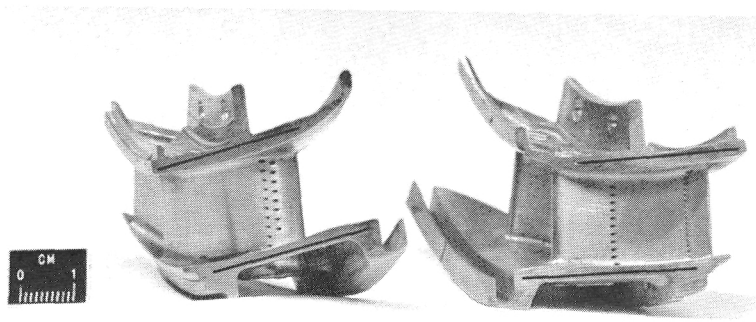

Figure 3. - Stator vane segments with coolant air ejection holes unplugged.

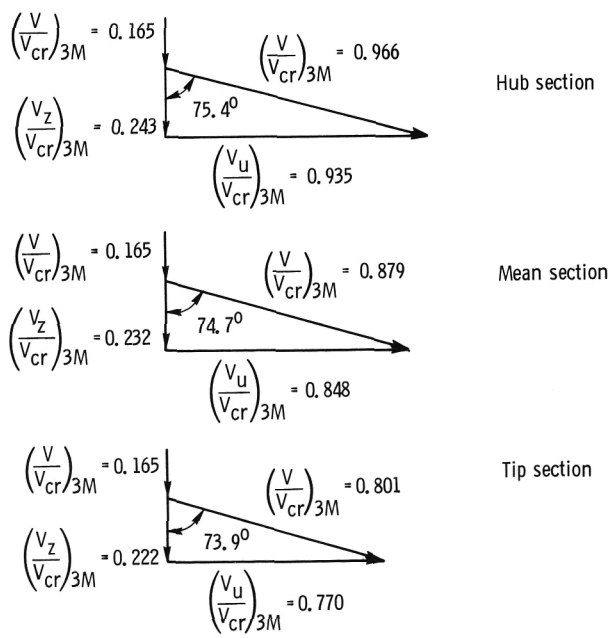

Figure 4. - Stator vane design velocity diagrams.

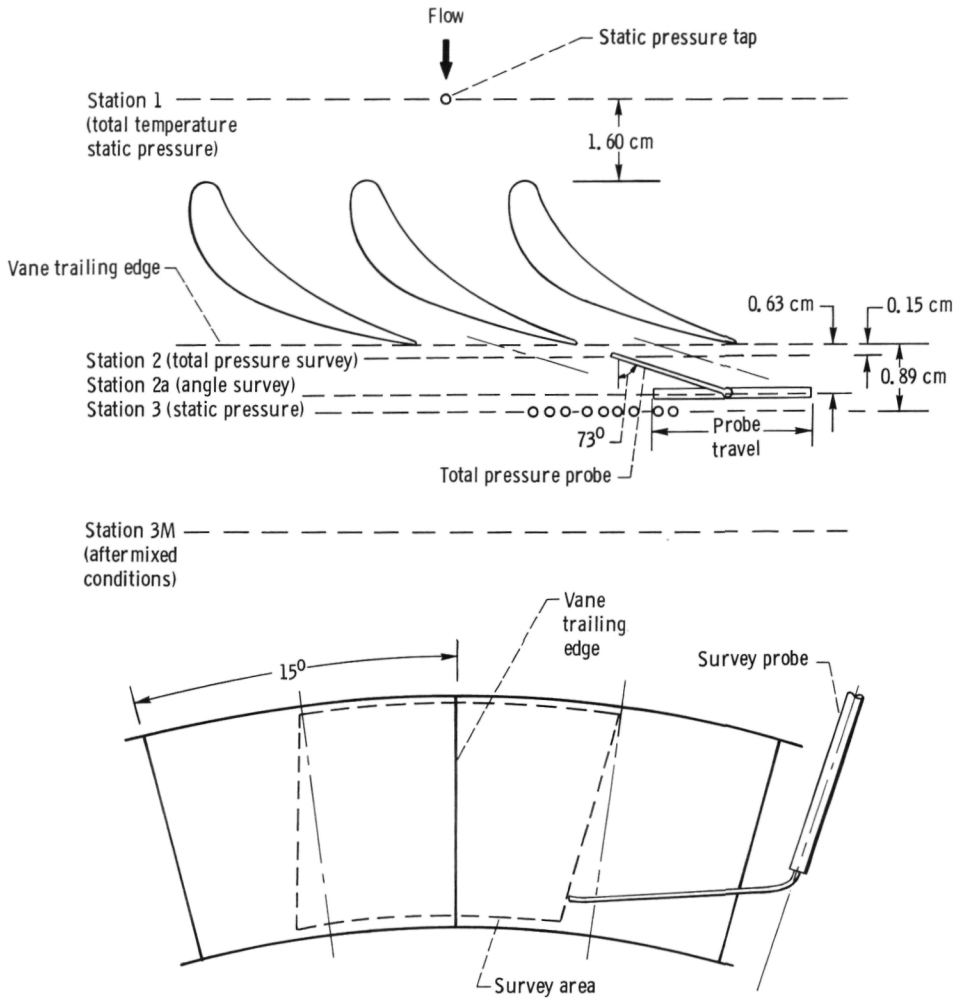

Figure 5. - Schematic of instrumentation for survey data.

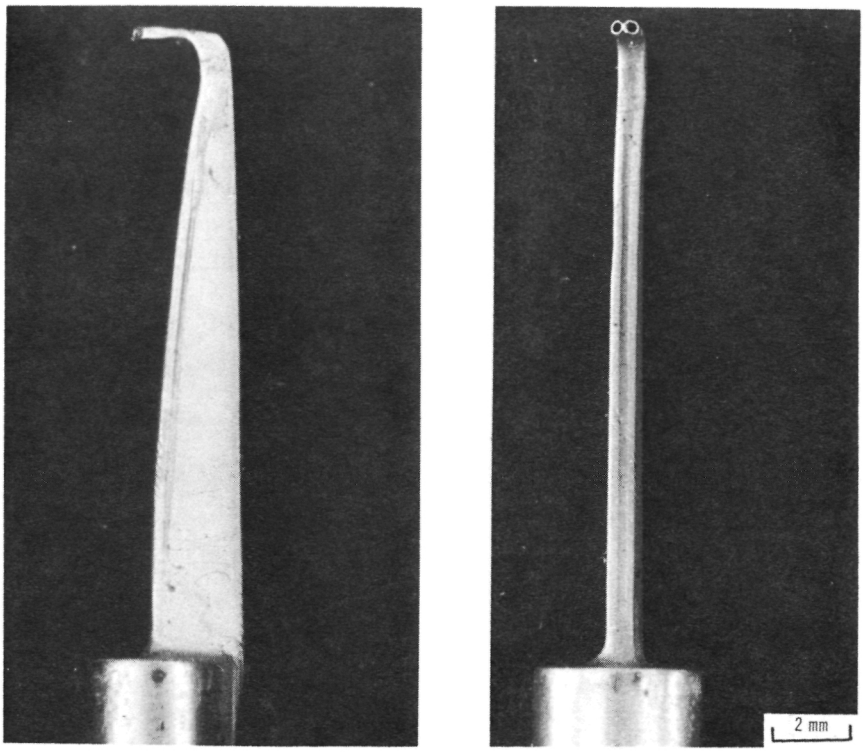

(a) Side view.

(b) Front view.

Figure 6. - Angle probe.

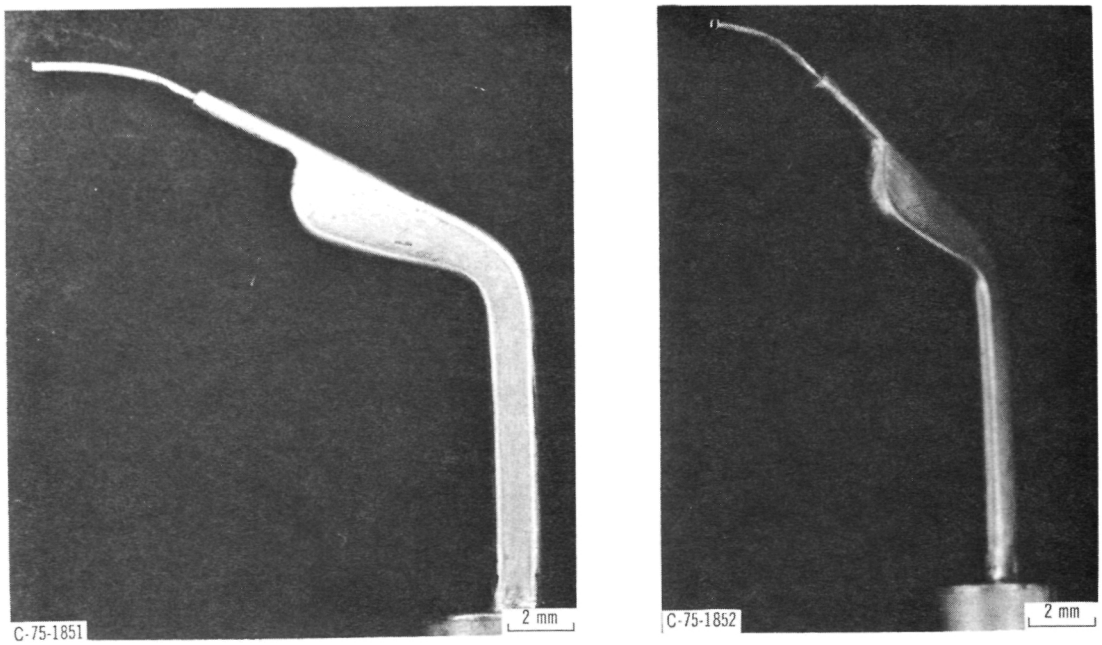

(a) Side view.

(b) Three-quarter front view.

Figure 7. - Total pressure survey probe.

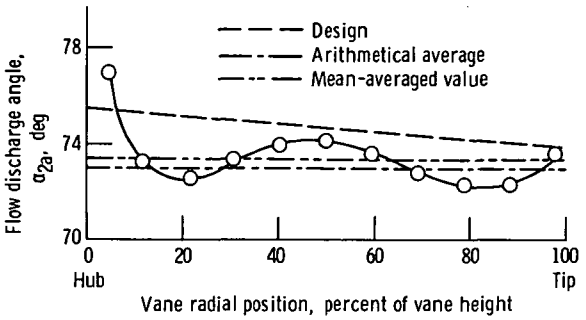

Figure 8. - Radial variation of flow discharge angle at mean-section ideal critical velocity ratio of 0.895.

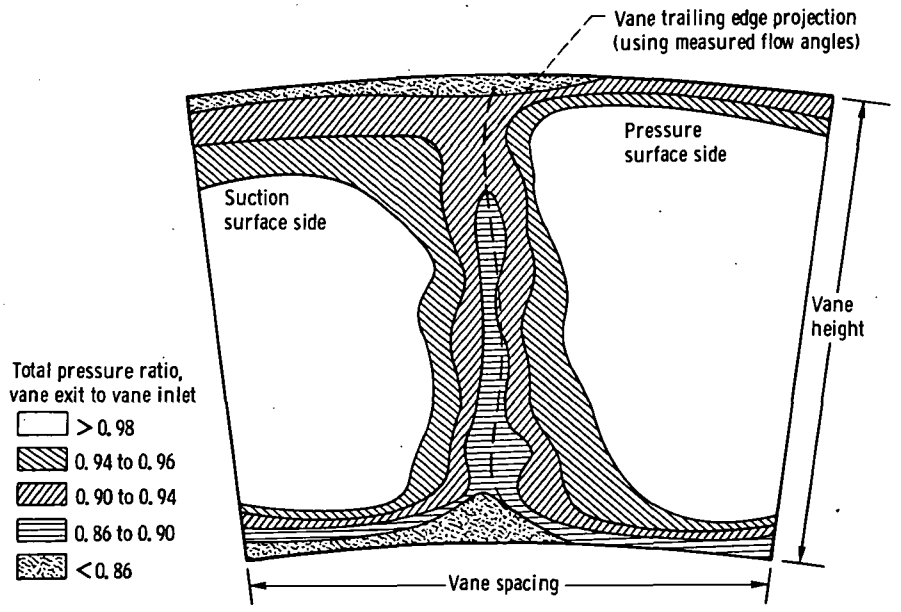

Figure 9. - Contours of total pressure at survey plane at mean-section ideal critical velocity ratio of 0.895.

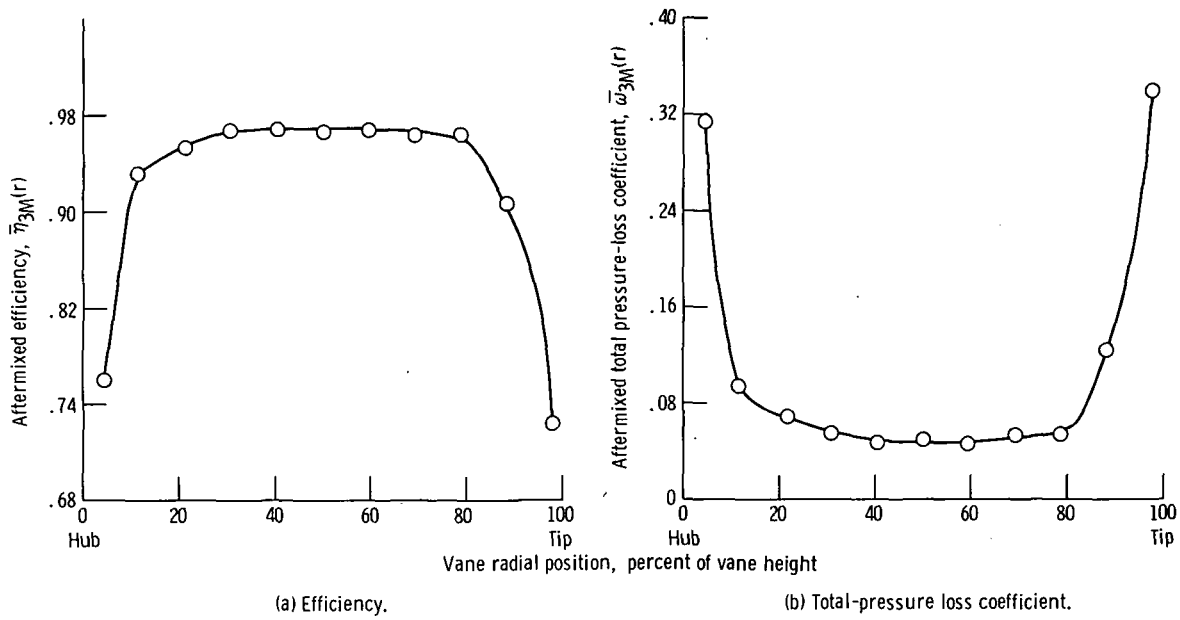

(a) Efficiency.

(b) Total-pressure loss coefficient.

Figure 10. - Radial variation of efficiency and total-pressure-loss coefficient at mean-section ideal critical velocity ratio of 0.895.

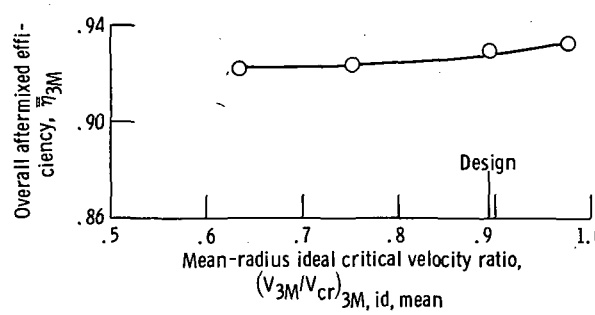

Figure 11. - Overall aftermixed efficiency and total-pressure-loss coefficient as functions of mean-section ideal critical velocity ratio.

NATIONAL AERONAUTICS AND SPACE ADMINISTRATION
WASHINGTON, D.C. 20546

OFFICIAL BUSINESS
PENALTY FOR PRIVATE USE $300

SPECIAL FOURTH-CLASS RATE
BOOK

POSTAGE AND FEES PAID
NATIONAL AERONAUTICS AND
SPACE ADMINISTRATION
451

U.S.MAIL

POSTMASTER : If Undeliverable (Section 158 Postal Manual) Do Not Return

"The aeronautical and space activities of the United States shall be conducted so as to contribute . . . to the expansion of human knowledge of phenomena in the atmosphere and space. The Administration shall provide for the widest practicable and appropriate dissemination of information concerning its activities and the results thereof."

—NATIONAL AERONAUTICS AND SPACE ACT OF 1958

NASA SCIENTIFIC AND TECHNICAL PUBLICATIONS

TECHNICAL REPORTS: Scientific and technical information considered important, complete, and a lasting contribution to existing knowledge.

TECHNICAL NOTES: Information less broad in scope but nevertheless of importance as a contribution to existing knowledge.

TECHNICAL MEMORANDUMS: Information receiving limited distribution because of preliminary data, security classification, or other reasons. Also includes conference proceedings with either limited or unlimited distribution.

CONTRACTOR REPORTS: Scientific and technical information generated under a NASA contract or grant and considered an important contribution to existing knowledge.

TECHNICAL TRANSLATIONS: Information published in a foreign language considered to merit NASA distribution in English.

SPECIAL PUBLICATIONS: Information derived from or of value to NASA activities. Publications include final reports of major projects, monographs, data compilations, handbooks, sourcebooks, and special bibliographies.

TECHNOLOGY UTILIZATION PUBLICATIONS: Information on technology used by NASA that may be of particular interest in commercial and other non-aerospace applications. Publications include Tech Briefs, Technology Utilization Reports and Technology Surveys.

Details on the availability of these publications may be obtained from:

SCIENTIFIC AND TECHNICAL INFORMATION OFFICE

NATIONAL AERONAUTICS AND SPACE ADMINISTRATION

Washington, D.C. 20546